

A simple model of the charge transfer in DNA-like substances

Niels R. Walet^{†§} and Wojtek J. Zakrzewski^{‡||}

[†] School of Physics and Astronomy, University of Manchester, P.O. Box 88, Manchester M60 1QD, UK

[‡] Dept. of Mathematical Sciences, University of Durham, Durham DH1 3LE, UK

Abstract. We present a very simple model for the study of charge transport in a molecule patterned on B-DNA. In this model we use a discrete non-linear Schrödinger equation to describe electrons propagating along the sugar-phosphate backbone of the DNA molecule. We find that in this model, for a given nonlinearity, the transport is controlled by J , a parameter which relates to the electronic coupling between the different molecules on the backbone. For smaller values of J we have localised states while at higher values of J the soliton field is spread out and through its interaction with the lattice it has stronger effects on the distortion of the lattice.

PACS numbers: 05.45.Yv, 87.15.Aa

1. introduction

As the molecule that carries all genetic information, DNA has been of great interest to chemists and physicists since before the unlocking of its structure by Watson and Crick [1], and both the structure and dynamics of the molecule have been investigated in great detail. Another key feature of DNA is the ease of its assembly as a linear macro-molecule of truly macroscopic scale; a potential realisation of a quantum wire (if it were a conductor). One can also use the DNA molecule as a scaffold to grow quantum wires, e.g., by deposition of conducting molecules in the minor groove.[2, 3, 4, 5]

With the experiments by Dekker and his group [6, 7, 8] on the conduction of single strands of DNA, and the controversy about the interpretation of the experiments, which suggested that DNA might be a conductor, a veritable floodgate for theoretical studies has opened. Most of these consider the conduction (or charge transport) along a one-dimensional “pi-stack” (a channel built from overlapping pi orbitals) in the centre of the DNA molecule.

Disregarding electronic transport, mathematical modelling of DNA has a long tradition, see for example the book Ref. [9]. In recent years the Peyrard-Bishop model (a simple two-dimensional model for DNA, which has been used successfully to describe the denaturing transition of that molecule) has become quite popular, see the review in [10] for a more complete set of references. Mingaleev *et al* [12, 11] have produced models which allow them to perform mathematical studies of DNA and its properties. This is an active field, and the number of relevant publications is large. The most relevant literature can be traced from a number of recent references, e.g., Refs. [13, 14, 15, 16, 17, 18, 19, 20, 21, 22, 23] and the review [24].

Recently one of the present authors (together with Dr. Hartmann) [25] looked at the model of Mingaleev *et al* and proposed a further generalisation of their one chain model to two chains. This two chain generalisation involved similar terms in the Lagrangian (for each chain) to those of the model of Mingaleev *et al* plus an extra term involving the interaction between the chains. The obtained results were encouraging, although due to the specific choice of terms, the numerical simulations were very slow.

In this note we reinvestigate these models and propose a new generalisation which, at least, has the advantage of fast numerical convergence. We use this model to investigate various aspects of DNA-like substances. Our model can be compared to the model used by Bishop *et al*. [22], but differs in many aspects. The two most crucial ones are the inclusion of the helicity of the molecule and the fact that in our model electrons are (correctly or incorrectly, that remains to be seen) allowed to propagate along the backbone rather than along the “pi-stack” of the overlapping molecular orbitals of the base pairs. The latter assumption is already quite old, and was first proposed by Eley [26] in 1962. In this work we concentrate our attention on the mathematical aspects of the problem postponing detailed aspects of the applicability of the model to real, physical and biological, systems to a further publication.

In the next section we say a few words about the DNA systems and in the following

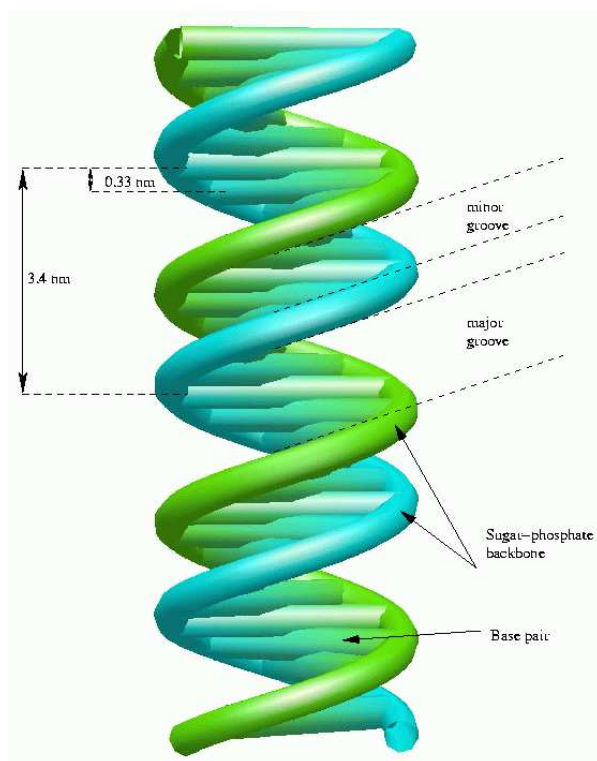


Figure 1. A schematic model of B-DNA

section we describe our ideas of how to build a model for DNA-inspired structures which can be used to describe such systems.

In the final section we describe in detail our first studies involving this model.

2. Some aspects of DNA

The basic structure of DNA varies quite considerably depending on its environment. B-DNA, the standard double helix, actually only occurs in aqueous solution. An idealised structure of DNA is given in figure 1.

We can easily see that each base pair advances the rotation of the chain by about 36° . The difference between the major and minor grooves is caused by the fact that the base-pairs are not exactly at right angles to the backbone. There is also a “propeller twist”: the plane of the base pairs is twisted like a propeller. See Ref. [27] for more details. As can be seen in the figure, the different base pairs are quite close in the centre of the molecule. This is why it is believed that DNA gains rigidity by overlapping pi-orbitals between the different base pairs. This same mechanism has been invoked in allowing charge transport through DNA.

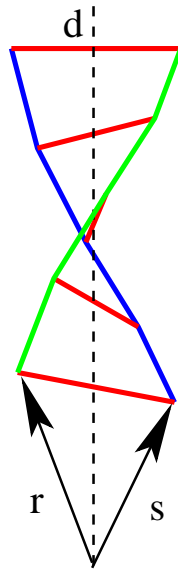


Figure 2. A simple model of a section of straight DNA

3. Modelling DNA

Our DNA model will consist of two parts: a simple classical model of a chiral molecule, that can twist and be locally compressed, but where we disregard the bending modes. This would be a natural approach to a stretched DNA molecule, attached between two electrical contacts. The situation is sketched schematically in figure 2 ¶. In that figure the thin (red) lines denote the hydrogen bonds, and are modelled to be at straight angles to the “virtual backbone” denoted by the dashed line. The thick (blue and green) lines denote the two DNA chains.

At the same time we assume electrons hop from a base pair to a base pair, occasionally moving from one side to the other. Our model for this process will be based on the discrete non-linear Schrödinger equation, which can be seen as the semi-classical limit of a tight-binding model.

We shall investigate the electronic model first, before concentrating on the molecular dynamics.

3.1. Electron dynamics

We assume a simple discrete non-linear Schrödinger equation for the movement of the electrons through DNA. We model the electron as hopping along sites labelled i , the position of a base on the back-bone. We have two electron fields, one on each ribbon, which we call ψ and ϕ (connected to the two sets of coordinates r and s described

¶ This may not be the best approach; stretching of the “rungs” may well be ignored at low temperatures, but the bending of the backbone seems to be a low-energy degree of freedom. For simplicity we do not model the very complicated bending and kinking [28].

above).

The action for the electrons, without coupling between the two chains, is taken to be

$$\mathcal{A} = \int dt \left\{ -\hbar \sum_i \psi_i^* \dot{\psi}_{i,t} - \hbar \sum_i \phi_i^* \dot{\phi}_{i,t} + \sum_i \left[\hbar\omega 2 |\psi_i|^2 - \sum_{j \neq i} J_{i-j} \psi_i^* \psi_j - \frac{1}{2} \chi |\psi_i|^4 \right] + \sum_i \left[\hbar\omega 2 |\phi_i|^2 - \sum_{j \neq i} J_{i-j} \phi_i^* \phi_j - \frac{1}{2} \chi |\phi_i|^4 \right] \right\} , \quad (1)$$

This can, for instance, be derived as the semi-classical limit of a tight-binding model, with a density-squared term added. Such non-linearities are crucial, since they limit the amount of charge that can collect at any one site. It is not obvious that such non-linearities are restricted to the on-site interaction, and we could also study the question “how different would the dynamics of the system be had we added an electronic term of the density-density correlation form $\sum_{i,j \neq i} \chi_{ij} |\psi_i|^2 |\psi_j|^2$?” We have no answer to this question - and we leave its resolution to some future work. In this paper we focus our attention on the study of the system essentially described by (1) together with a further potential describing the interchain interaction. As we shall see this system is already sufficiently complicated to exhibit many interesting properties.

3.2. The interaction between chains

Of course, one of the key elements of the problem is the interaction between the chains (and we limit ourselves to consider only the interaction between the two nearest sites on the backbones, i.e. $i = j$). The most naive choice of such an interaction is to take

$$V_{\text{int}} = \sum_i K (\phi_i^* \psi_i + \psi_i^* \phi_i) . \quad (2)$$

This form of the interchain interaction term is actually rather uninteresting since it leads to a simple oscillation of charges from one strand to the other, while their combination behaves as a single unit, and we would thus reproduce the usual results of the discrete nonlinear Schrödinger Equation (DNLS)⁺.

This is due to the fact that Eq. (2) does not take into account the chirality of the molecules. A possible improvement would involve making the coupling orientation dependent:

$$V_{\text{int}} = \sum_i K (e^{i2g\theta_i} \phi_i^* \psi_i + e^{-i2g\theta_i} \psi_i^* \phi_i) , \quad (3)$$

(where g is yet another parameter). Here θ_i is the angle of the i sites on the backbones relative to some arbitrary direction (see later). This is not satisfactory, however, since

⁺ For a good description of properties of this model see e.g. [29].

for a flat molecule the tunnelling would now depend on its orientation! We can think of two further improvements:

First of all we can subtract the average orientation,

$$V_{\text{int}} = \sum_i K(e^{i2g(\theta_i - \langle \theta \rangle)} \phi_i^* \psi_i + e^{-i2g(\theta_i - \langle \theta \rangle)} \psi_i^* \phi_i) \quad , \quad (4)$$

which leads to a rather non-local coupling. This rather artificial approach will not be further investigated in this work, since it is not related to the chirality of the DNA molecule.

Secondly, we can invert the transformation of fields obtained from going from Eq. (2) to Eq. (3), which corresponds to a gauge-like transformation of the naive interaction, Eq. (2). This implies that we should make the replacement

$$\psi_i \rightarrow e^{ig\theta_i} \psi_i, \quad \phi_i \rightarrow e^{-ig\theta_i} \phi_i \quad (5)$$

everywhere (i.e., also in all the interaction terms within each one of the backbones). For a flat molecule this has no consequence, and the orientation dependence of Eq. (3) disappears, but for a curved molecule, as we shall show below, this indeed includes effects due to chirality.

Our modification then implies that we can use Eq. (2), but must replace the non-local interaction along the backbone by

$$\sum_{i,j \neq i} J_{i-j} (\psi_i^* \psi_j + \phi_i^* \phi_j) \rightarrow \sum_{i,j \neq i} J_{i-j} (e^{ig(\theta_j - \theta_i)/2} \psi_i^* \psi_j + e^{-ig(\theta_j - \theta_i)/2} \phi_i^* \phi_j) \quad . \quad (6)$$

This is obviously rotationally invariant.

3.3. Continuum limit and chirality

Let us look at the continuum limit of

$$\sum_{i,j} J_{|i-j|} e^{ig(\theta_j - \theta_i)} \psi_i^* \psi_j \quad (7)$$

and

$$\sum_{i,j} J_{|i-j|} e^{-ig(\theta_j - \theta_i)} \phi_i^* \phi_j, \quad (8)$$

in order to see that this expression really describes a chiral molecule. The second term is simply related to the first by the replacement $\theta_i \rightarrow -\theta_i$ and $\psi \rightarrow \phi$. We thus concentrate on the first term, where we assume that $J_{|i|}$ falls sufficiently fast so that we need consider only the nearest-neighbour terms. Calling the contribution of these terms, divided by J_1 , k_1 , we find that

$$k_1 = \sum_i (\psi_i^* \psi_{i+1} e^{ig(\theta_{i+1} - \theta_i)} + \text{c.c.}) \quad (9)$$

Next we assume that $\theta_{i+1} - \theta_i$ is small and we expand k_1 to first order in this quantity. Before doing so, we introduce some time-saving notation,

$$(\delta f)_i = \frac{f_{i+1/2} - f_{i-1/2}}{h}, \quad \langle f \rangle_i = \frac{f_{i+1/2} + f_{i-1/2}}{2}. \quad (10)$$

Let's now expand and simplify k_1

$$\begin{aligned}
 k_1 &= \sum_i (\psi_i^* \psi_{i+1} (1 + ig(\delta\theta)_{i+1/2}) + \text{c.c.}) \\
 &= \frac{1}{2} \sum_i (\psi_i^* (\psi_{i+1} + \psi_{i-1} + \text{c.c.}) \\
 &\quad + \frac{g}{2} \sum_i (i\psi_i^* (\psi_{i+1}(\delta\theta)_{i+1/2} + \psi_{i-1}(\delta\theta)_{i-1/2}) + \text{c.c.}) \\
 &= \frac{\hbar^2}{2} \sum_i (\psi_i^* (\delta^2\psi)_i + \text{c.c.}) + \sum_i |\psi_i|^2 \\
 &\quad + \hbar \frac{g}{2} \sum_i (i\psi_i^* (\langle\psi\rangle_{i+1/2}(\delta\theta)_{i+1/2} - \langle\psi\rangle_{i-1/2}(\delta\theta)_{i-1/2}) + \text{c.c.}) \\
 &= \frac{\hbar^2}{2} \sum_i (\psi_i^* (\delta^2\psi)_i + \text{c.c.}) + \sum_i |\psi_i|^2 \\
 &\quad + \hbar^2 \sum_i \left(\psi_i^* \left(\delta \left[\langle\psi\rangle (i \frac{g}{2} \delta\theta) \right] \right)_i + \text{c.c.} \right). \tag{11}
 \end{aligned}$$

If we combine the ‘onsite’ term $|\psi_i|^2$ in a similar term already present in the model, we find that the remaining terms become

$$\begin{aligned}
 k_1/h &= \frac{1}{2} \int dx (\psi^* \partial_x (\partial_x + igA)\psi + \psi \partial_x (\partial_x - igA)\psi^*) \\
 &\approx - \int dx ((D_x\psi)^* D_x\psi). \tag{12}
 \end{aligned}$$

Here $A = \partial_x \theta$, $D_x = \partial_x + igA$. In the last step we have added a second order term in θ (neglected in our initial evaluation). Thus we end up with a covariant derivative. The other chain (ϕ) contains the complex conjugate covariant derivative,

$$k_1^\phi \approx - \int dx ((D_x^*\phi)^* D_x^*\phi). \tag{13}$$

Thus we see that with this structure of the coupling to a ‘magnetic flux’ caused by the warping of the molecule through each plaquette, we have indeed constructed a chiral model of electrons moving through a molecule.

3.4. Solitons in a curved background

First we shall study the discrete solitons (breathers) of the model, i.e., solutions of the form $\psi_i = e^{i\Omega t} f_{-1,i}$, $\phi_i = e^{i\Omega t} f_{1,i}$. We assume that the distance between the molecules is specified by the parameters $d = 2.39$ nm, $\delta z = 3.38/10 = 0.338$ nm, $\delta\theta = 2\pi/10 = 0.628$.

This leads to the non-linear eigenvalue problem

$$2\hbar\omega f_{k,i} - \sum_{j \neq i} e^{ig\lambda(\theta_j - \theta_i)/2} J_{i-j} f_{\lambda,j} - \chi |f_{\lambda,i}|^2 f_{\lambda,i} + K f_{\bar{\lambda},i} = \hbar\Omega f_{\lambda,i} \quad , \tag{14}$$

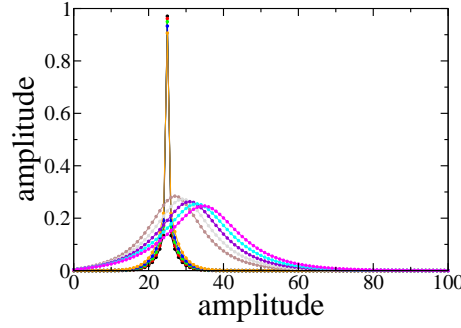


Figure 3. The profile of the DNLS breather for various values of the coupling constant J_0 , starting from $J_0 = 0.22$ and a solution localized at $i = 25$, increasing J_0 in steps of 0.02. The transition occurs between $J_0 = 0.3$ and $J_0 = 0.32$. Wider curves represent larger values of J_0 .

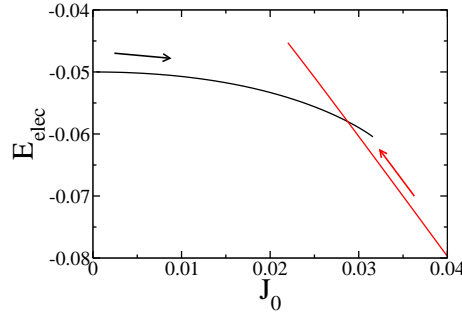


Figure 4. The transition between solitonic and delocalised solutions as a function of the coupling constant J_0 .

where the term containing $\bar{\lambda} = -\lambda$ denotes the coupling to the other chain. One of the ways this problem can be solved is through a constrained minimization, with $\hbar\Omega$ being the Lagrange multiplier imposing charge normalisation.

We have studied the nature of such solutions, for $\hbar\omega = 1$, $J_{i-j} = J_0 e^{-\beta d_{ij}}$, $\chi = 0.1$ and $\kappa = 1$. We have found that the coupling between the two chains leads to solitons that are distributed evenly over the two backbones, but where the phase varies.

If we ignore the coupling between the two strands of the double helix for a while, and analyse the motion of a single electron along an equilibrium chain, we are essentially solving the DNLS, and the interesting solutions are breathers of the form $\phi_i(t) = e^{i\omega t} f_i$ [29]. These can be found quite easily for the current model by a simple steepest descent method (minimizing the electronic energy). In figure 3 we present the profiles of the DNLS breather for various values of the coupling constant J_0 . In our simulations we have found a sharp transition from a localised to delocalised solution for values of J_0 about 0.0282. As can be seen from figure 4 the transition appears to be of first order, and the solutions are metastable beyond the transition.

When we increase the coupling we find that it is instructive to look in more detail at the energetics of the problem, as shown in figure 5, where $\beta = 1\text{nm}^{-1}$ and various

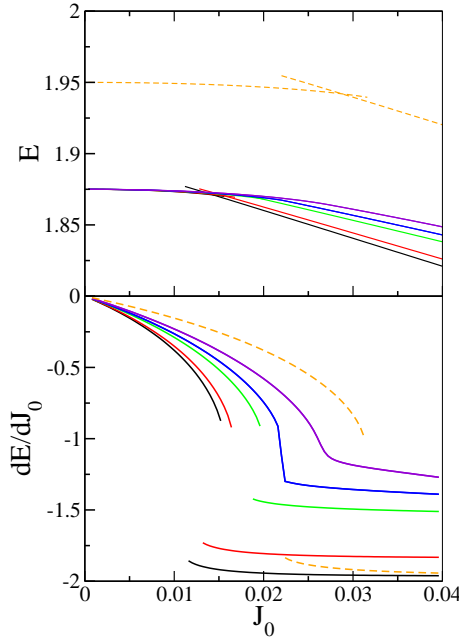


Figure 5. The energy (mass) of the breather for two coupled chains, as a function of the coupling constant J_0 , and $\beta = 1\text{nm}^{-1}$. From bottom to top, the curves correspond to: black $g = 0$, red $g = 0.5$, green $g = 1$, blue $g = 1.2$ and violet $g = 1.5$. The dashed (orange) curves show the single chain solution from above. In each case we have performed our calculations for both the increasing and decreasing J_0 .

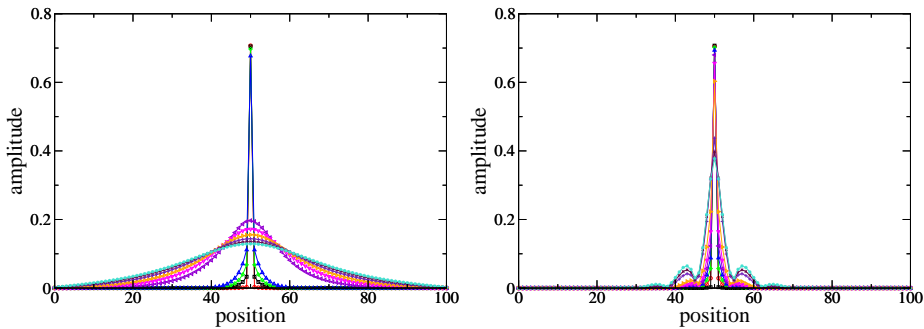


Figure 6. The profile of the DNLS breathers as a function of the coupling constant of the coupling constant J_0 , and $\beta = 1\text{nm}^{-1}$. The left figure shows $g = 0$, the right one $g = 1.5$. The sharpest curves occur for the smallest value of J_0 , with a sequential broadening on increase.

values of g have been used. We still see the phase transition, but note that there is a shift in the position, and that it seems to change from first to second or higher order with increasing chiral charge g . As can be seen in figure 6, there is a change in the nature of the solitonic positions as well, and we are no longer able to find fully delocalised ones. If we increase β the transition seems to weaken even more, and the solitons seem to sharpen; see figures 7 and 8.

If we wish to study the mobility of the solitons, moving breathers, etc the

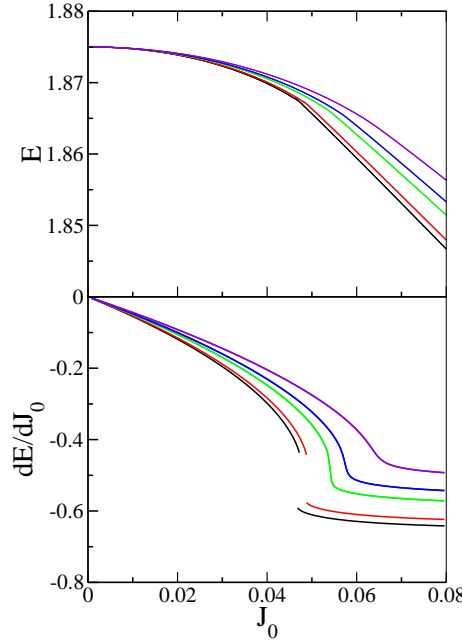


Figure 7. The energy (mass) of the breather for two coupled chains, as a function of the coupling constant J_0 , and $\beta = 2\text{nm}^{-1}$. From bottom to top, the curves correspond to: black $g = 0$, red $g = 0.5$, green $g = 1$, blue $g = 1.2$ and violet $g = 1.5$. In each case we have performed our calculations for both the increasing and decreasing J_0 .

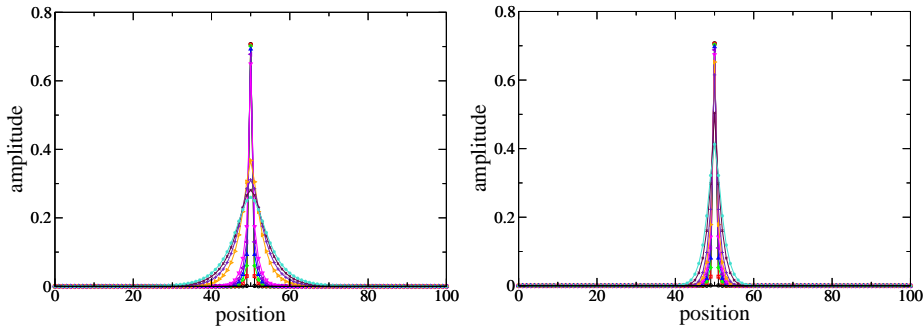


Figure 8. The profile of the DNLS breathers as a function of the coupling constant J_0 , and $\beta = 2\text{nm}^{-1}$. The left figure shows $g = 0$, the right one $g = 1.5$. The sharpest curves occur for the smallest value of J_0 , with a sequential broadening as J_0 increases.

standard technique [29] in the field suggests the use of the smooth-profile (continuum) approximation, where we have added a term of the form

$$iv(f_{\lambda,i+1} - f_{\lambda,i-1})/2 \quad (15)$$

to the left hand-side of the eigenvalue problem. Results of such calculations are given in figures 9 and 10. Here the phase transition probably plays an important role as for small J_0 we have a very localised solution which strongly violates the continuum approximation. In this case we are unable to find a moving soliton. For larger values of J_0 we do find a smooth profile solution, which suggests that we have found the moving

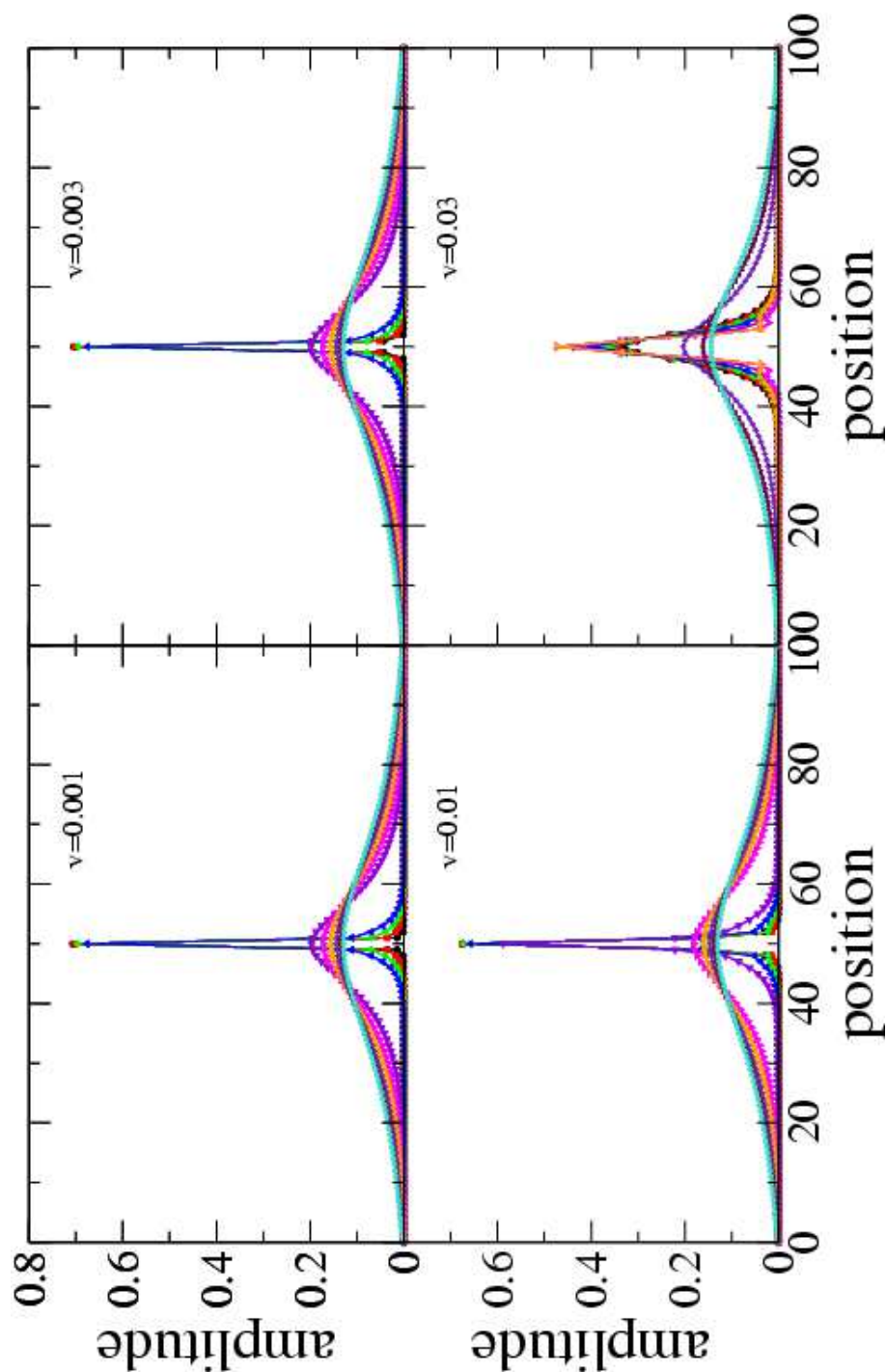


Figure 9. The shape of the moving breather for two coupled chains, as a function of the coupling constant J_0 , $g = 0$ and $\beta = 2\text{nm}^{-1}$. The sharpest curves occur for the smallest value of J_0 .

soliton. This we expect to have an important impact on the charge transport properties of the system. Generally, the effect of the chirality of the molecule seems to sharpen the profile thus reducing the mobility!

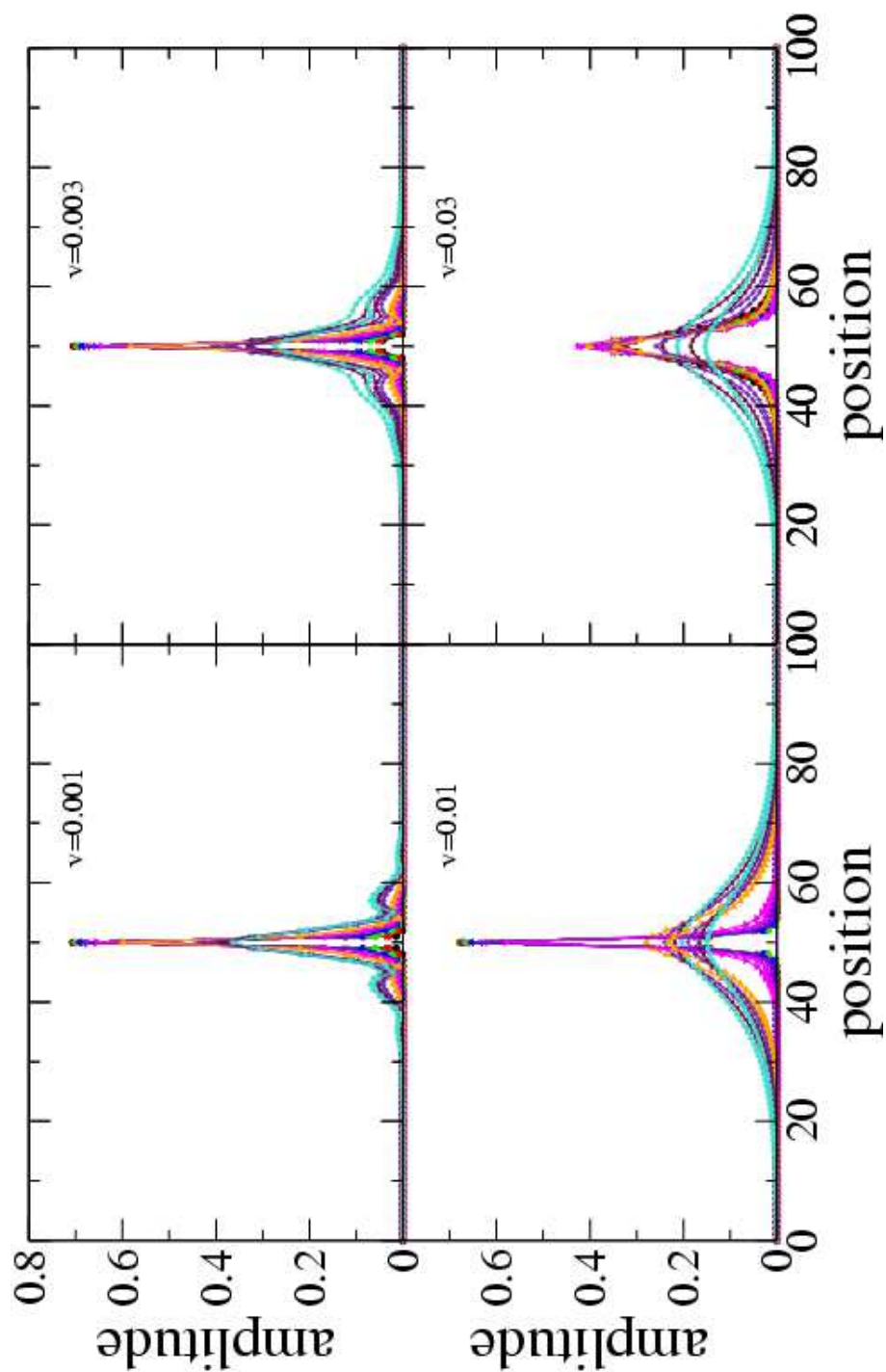


Figure 10. The shape of the moving breather for two coupled chains, as a function of the coupling constant J_0 , $g = 1.5$ and $\beta = 2\text{nm}^{-1}$. The sharpest curves occur for the smallest value of J_0 broadening as J_0 increases.

3.5. The molecule

The model for the molecule can be specified in its most general form by solving a number of constraints, which we shall try to parametrise in as simple a way as possible. Looking at the figure, it seems easy to work with the following representation: (we use \mathbf{r}_i to denote the position where the i th base pair is attached to one of the chains, \mathbf{s}_i for the other one)

$$\mathbf{r}_i = z_i \mathbf{e}_z + \frac{1}{2} d \mathbf{u}_i, \quad \mathbf{s}_i = z_i \mathbf{e}_z - \frac{1}{2} d \mathbf{u}_i, \quad (16)$$

with \mathbf{u} a 2D unit vector in the xy plane. Hence it is natural to relate the angles θ_i introduced in (3) to the orientation of \mathbf{u}_i in the xy plane. Our representation makes it possible to allow for stretching of the H bonds by adding a potential for d (as in the Peyrard-Bishop model). We shall use a molecular potential to implement an approximate constraint on the spacing in the strands of DNA, but it is not so straightforward to study the effect of bending of the double helix in this model, which could be quite important [28].

The kinetic energy is relatively easy to evaluate

$$\begin{aligned} \frac{1}{2} M \sum_i \mathbf{r}_{i,t}^2 + \mathbf{s}_{i,t}^2 &= \frac{1}{2} M \sum_i \left(z_i \mathbf{e}_z + \frac{1}{2} d \mathbf{u}_i \right)_t^2 + \left(z_i \mathbf{e}_z - \frac{1}{2} d \mathbf{u}_i \right)_t^2 \\ &= M \sum_i \left(z_{i,t}^2 + \frac{1}{4} d^2 \mathbf{u}_{i,t}^2 \right) . \end{aligned} \quad (17)$$

We can easily generalise this to a dynamical d ; in this case the length of each rung becomes $d_i(t)$, and the additional terms in the kinetic energy would be of the form $\frac{1}{4} d_{i,t}^2$. However, we expect the effects of the variation of d to be small, so in this work we will keep d fixed.

We shall now describe a set of simple potentials, all corresponding to properties of the bonds or the angles between bonds, that can be used to describe equilibrium DNA.

If we insist on a molecule where the equilibrium shape is bent, such as DNA, we must impose an equilibrium angle between the bonds. One such potential would be

$$\begin{aligned} U_B \propto \sum_i & \left[((\mathbf{r}_i - \mathbf{r}_{i-1}) \times (\mathbf{r}_{i+1} - \mathbf{r}_i))^2 - \alpha_s^2 \right]^2 \\ & + \left[((\mathbf{s}_i - \mathbf{s}_{i-1}) \times (\mathbf{s}_{i+1} - \mathbf{s}_i))^2 - \alpha_s^2 \right]^2 . \end{aligned} \quad (18)$$

Actually, this is too simple. In turning the outer product into a scalar, we have now allowed mixing of the left- and right-handed turns in the same molecule. Since DNA is a chiral molecule, we would like to add a term that prefers left-handed over right-handed twists. This is most easy to construct the continuum limit, where this translates into the requirement that the vector tangential to one of the strands points both upwards and into the plane, or in the opposite direction (downwards and out of the plane). Suppose that the point on the strand is specified by a vector $\boldsymbol{\delta}$ from the back bone (i.e., $\boldsymbol{\delta}$ lies in the xy plane), we write $\boldsymbol{\delta} = \delta \mathbf{e}$ (in the notation used above, $\mathbf{e} = \pm \mathbf{u}$, depending on

which strand we are on), with

$$\mathbf{e} = (\cos \theta, \sin \theta, 0). \quad (19)$$

We can then write for the tangent vector

$$\mathbf{t} = a(-\sin \theta, \cos \theta, 0) + b(0, 0, 1), \quad (20)$$

and, to introduce chirality, we wish to add a bias towards a particular value of ab in our model. We can extract a by calculating $\mathbf{e}_z \cdot (\mathbf{e} \times \mathbf{t})$, and $b = \mathbf{e}_z \cdot \mathbf{t}$. Replacing \mathbf{t} by the discrete analogue $\mathbf{r}_{i+1} - \mathbf{r}_i$, we find that

$$\begin{aligned} a_r &\approx \mathbf{e}_z \cdot \left[\frac{1}{2}(\mathbf{u}_i + \mathbf{u}_{i+1}) \times \left((z_{i+1} - z_i)\mathbf{e}_z - \frac{d}{2}(\mathbf{u}_{i+1} - \mathbf{u}_i) \right) \right] \\ &= \frac{d}{2} \mathbf{e}_z \cdot (\mathbf{u}_{i+1} \times \mathbf{u}_i) \quad , \end{aligned} \quad (21)$$

$$\begin{aligned} b_r &\approx \mathbf{e}_z \cdot \left((z_{i+1} - z_i)\mathbf{e}_z - \frac{d}{2}(\mathbf{u}_{i+1} - \mathbf{u}_i) \right) \\ &= z_{i+1} - z_i \quad . \end{aligned} \quad (22)$$

Here, due to the symmetry, $a_s = a_r$ and $b_s = b_r$. A potential that achieves our aim is of the form

$$U_B = \sum_i g_\mu((z_{i+1} - z_i)\mathbf{e}_z \cdot (\mathbf{u}_{i+1} \times \mathbf{u}_i)) \quad , \quad (23)$$

with g a function that has a minimum at μ , the chosen average parameter, and increases quickly as we move away from equilibrium. An example of such a function which in fact we have used in our simulations, is

$$g(x) = b(x - \mu)^2. \quad (24)$$

We will also assume that each of the back-bones (the strands) can stretch; this will be built into our model by introducing a stretching potential of the bonds of the form (note that stretching for the other strand is constrained by the symmetry imposed by the straightness of our molecule)

$$\begin{aligned} U_s &= \sum_i f_l(|\mathbf{r}_i - \mathbf{r}_{i+1}|^2) \\ &= \sum_i f_l^2((z_{i+1} - z_i)^2 + \frac{d^2}{2}(1 - \mathbf{u}_{i+1} \cdot \mathbf{u}_i)) \quad , \end{aligned} \quad (25)$$

where f is has a minimum at the average distance l^2 , and increases quickly away from the minimum. As f describes a stretching potential we can either use a harmonic potential, $f(x) = a(x - l^2)^2$, or a Morse potential, $f(x) = a(e^{-(x-l^2)^{1/2}} - 1)^2$. In our simulations we have used the simple quadratic form

$$f(x) = a(x - l^2)^2 \quad (26)$$

3.6. A small simplification

Before we proceed further we note that we can simplify the problem slightly by using a 1D angle representation for \mathbf{u} ,

$$\mathbf{u}_i = (\cos \theta_i, \sin \theta_i, 0) \quad . \quad (27)$$

We then find

$$\mathbf{u}_{i,t}^2 = \dot{\theta}_i^2 \quad , \quad (28)$$

and

$$U_B = \sum_i g_\mu((z_{i+1} - z_i) \sin(\theta_{i+1} - \theta_i)) \quad , \quad (29)$$

as well as

$$U_s = \sum_i f_2((z_{i+1} - z_i)^2 + \frac{d^2}{2}(1 - \cos(\theta_{i+1} - \theta_i))) \quad . \quad (30)$$

Next we determine the equations of motion for all the fields of our system. They are given by:

$$-\hbar i \psi_{i,t} = -2\hbar \omega \psi_i + \sum_{j \neq i} J_{i-j} \psi_j + \frac{1}{2} \chi \psi_i^2 \psi_i^* + K \phi_i \quad , \quad (31)$$

$$\begin{aligned} \frac{d^2}{2} M \ddot{\theta}_i = & + g'((z_{i+1} - z_i) \sin(\theta_{i+1} - \theta_i))(z_{i+1} - z_i) \cos(\theta_{i+1} - \theta_i) \\ & - g'((z_i - z_{i-1}) \sin(\theta_i - \theta_{i-1}))(z_i - z_{i-1}) \cos(\theta_i - \theta_{i-1}) \\ & + f'((z_{i+1} - z_i)^2 + \frac{d^2}{2}(1 - \cos(\theta_{i+1} - \theta_i))) \frac{d^2}{2} \sin(\theta_{i+1} - \theta_i) \\ & - f'((z_{i-1} - z_i)^2 + \frac{d^2}{2}(1 - \cos(\theta_i - \theta_{i-1}))) \frac{d^2}{2} \sin(\theta_i - \theta_{i-1}) - \alpha \dot{\theta}_i \\ & + \text{terms depending on } J \end{aligned} \quad (32)$$

and

$$\begin{aligned} 2M \ddot{z}_i = & + g'((z_{i+1} - z_i) \sin(\theta_{i+1} - \theta_i)) \sin(\theta_{i+1} - \theta_i) \\ & - g'((z_i - z_{i-1}) \sin(\theta_i - \theta_{i-1})) \sin(\theta_i - \theta_{i-1}) \\ & + f'((z_{i+1} - z_i)^2 + \frac{d^2}{2}(1 - \cos(\theta_{i+1} - \theta_i))) 2(z_{i+1} - z_i) \\ & - f'((z_i - z_{i-1})^2 + \frac{d^2}{2}(1 - \cos(\theta_i - \theta_{i-1}))) 2(z_i - z_{i-1}) - \alpha \dot{z}_i \\ & + \text{terms depending on } J \quad . \end{aligned} \quad (33)$$

Please note that we have added a damping term to both the z and θ equations (the term proportional to α). This helps us to lower the energy in our system and to determine its lowest energy states which will be solitonic if the system possesses such solutions.

The only remaining question is the choice of g . A sensible choice seems to be: $g_\mu(x) = b(x - \mu)^2$ and this is the expression we used in our simulations.

3.7. J dependence

Next we add the J dependent terms which will control electron's mobility. Although, in principle, J can depend on many variables two obvious dependences first spring to mind:

- (i) The tunnelling rate is a function of the shortest distance between two spatial points, i.e., $r_{ij} = |\mathbf{r}_i - \mathbf{r}_j|$, or
- (ii) The tunnelling rate depends on the distance along the DNA backbone (the sucrose molecules), $r_{ij} = \sum_{k=i}^{j-1} |\mathbf{r}_i - \mathbf{r}_{i+1}|$.

The first case is obviously easier to implement, but shall not be used in this work,

The second case is more complicated. Nonetheless; we can write $J_{ij} = h(R_{ij})$ and find that the additional terms in the EoM for θ , Eq. (32) are of the form

$$\begin{aligned}
& - \frac{d^2 \sin(\theta_{i+1} - \theta_i)}{r_{i+1,i}} \sum_{k \leq i, l > i} h'(R_{kl}) \psi_k^* \psi_l + (k \leftrightarrow l) \\
& - \frac{d^2 \sin(\theta_{i-1} - \theta_i)}{r_{i-1,i}} \sum_{k < i, l \geq i} h'(R_{kl}) \psi_k^* \psi_l + (k \leftrightarrow l)
\end{aligned} \tag{34}$$

and for z (Eq. (33))

$$\begin{aligned}
& - \frac{d^2 z_i (z_i - z_{i+1})}{r_{i+1,i}} \sum_{k \leq i, l > i} h'(R_{kl}) \psi_k^* \psi_l + (k \leftrightarrow l) \\
& - \frac{d^2 z_i (z_i - z_{i-1})}{r_{i-1,i}} \sum_{k < i, l \geq i} h'(R_{kl}) \psi_k^* \psi_l + (k \leftrightarrow l) \quad .
\end{aligned} \tag{35}$$

3.8. Choice of parameters

Next we attempt to determine the realistic (i.e. of some relevance in biophysics) range of our parameters. First we look at the static solutions of the ‘‘molecular’’ part of the energy, and minimise both the bending and the stretching potentials; we find that

$$(z_{i+1} - z_i) \mathbf{e}_z \cdot (\mathbf{u}_i \times \mathbf{u}_{i+1}) = \mu \quad , \tag{36}$$

$$(z_{i+1} - z_i)^2 - \frac{d^2}{2} \mathbf{u}_{i+1} \cdot \mathbf{u}_i = l^2 - \frac{d^2}{2}. \tag{37}$$

Assuming uniformity we get

$$\delta z \sin \delta \theta = \mu \quad , \tag{38}$$

$$\delta z^2 + d^2 \sin^2(\delta \theta / 2) = l^2 \quad , \tag{39}$$

where $\delta z = (z_{i+1} - z_i)$, $\delta \theta$ is the angle between two subsequent \mathbf{u} 's. Thus it is simple to find a value for μ and l given δz , d and $\delta \theta$, which we take from the studies of the real DNA. The standard values are [27]

$$d = 2.39 \text{ nm} \quad , \tag{40}$$

$$\delta z = 3.38/10 = 0.338 \text{ nm} \quad , \tag{41}$$

$$\delta \theta = 2\pi/10 = 0.628 \quad . \tag{42}$$

This gives us

$$\mu = 0.20 \text{ nm}, \quad l = 0.81 \text{ nm} \quad . \quad (43)$$

If we look at all the minima for these values of μ , l and d we find that we have a second solution

$$\delta z = 0.746 \text{ nm}, \quad \delta \theta = 0.858 \quad ; \quad (44)$$

this indicates an obvious weakness of our model—it will lead to coexisting shapes!

4. Numerical Studies

We have performed several numerical studies of our system. We have taken sensible parameters; i.e. those that appeared not to be completely inconsistent with the natural physical constraints but, at the same time, are quite useful to gain some understanding of the nature of the solutions. We have taken $\hbar = M = 1$, $\omega = 1$ (1), $a = 6$, $l^2 = 0.7$ (26), $b = 6$, $\mu = 0.2$ (24), $K = 0.1$ (3). The damping for the molecular motion was set at $\alpha = 0.02$. We also varied the value of J from 0.01 to 10.

We have found that for small values of J the system behaved in a sensible way - i.e., the molecules were quite rigid and the electron field modified their behaviour very little. The electron field was solitonic in nature and it affected the molecule primarily in the places where it was nonzero. For larger values of J —i.e., $J > 0.035$ the electron field dispersed and its effects were more pronounced. This can be most easily seen by looking at the figures which we include. To obtain them we used a 101 “rung” model of the twisted DNA-ladder, i.e., with 10 complete turns. We note that the transition point from the localised to the delocalised regime appears to have moved a bit as compared to the DNLS, see below.

In our first simulations we looked at $J = 0.02$. As can be seen from figure 11, in this case, the kinetic energy decayed rapidly, and so did the potential, leaving us with a breather soliton, see figure 12.

In this figure we show that the amplitude (square-root of the probability) of the electron field at one rung (i.e. summed over the two sites connected by that rung) performs semi-regular oscillations. The simulation was started out with all probability on one site of one backbone. We note also that some probability starts propagating outwards. This is then reflected from the boundaries, returns to the soliton and makes the breather’s oscillations somewhat less periodic resulting in a small sea of background oscillations.

Some aspects of the periodicity can also be seen in figure 13 where we have plotted the time dependence of the total probability on one of the two backbones (i.e. summed over all 101 sites on that backbone). We observe a fast decay to 0.5, and then small oscillations around this value, related to the periodicity of the breather.

We note that the presence of the soliton leads to a pronounced deviation of θ and z from their equilibrium values, with a sharp jump at the position of the soliton (figure 14). There seems to be a stronger correlation between these two quantities than one would

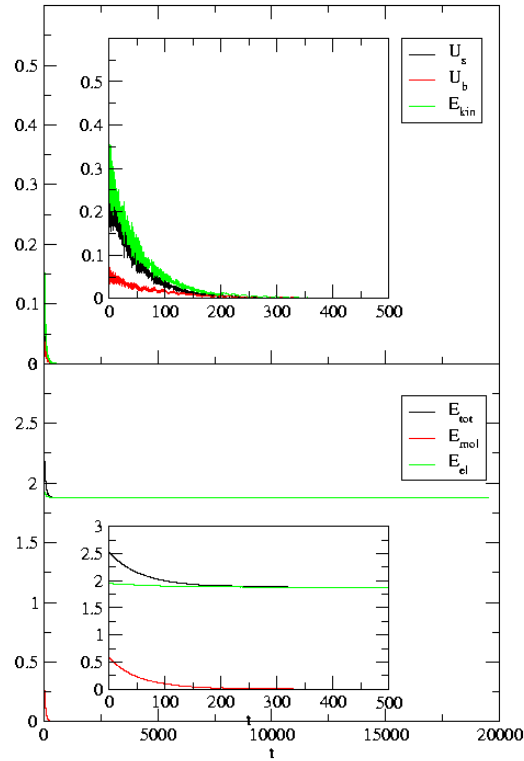


Figure 11. Energetics of the relaxation of a 101-rung chain for $J = 0.02$. The upper panel with inset shows the decrease of the mechanical energy, and the lower panel the same for the total and electronic energy

have naively expected, but the overall picture shows that there is a deformation and relaxation of the double helix.

Next we have studied a transitional case, namely, $J = 0.03$.

Once again the relaxation to the equilibrium has been quick and uneventful, at least as far as the energies are concerned, see figure 15.

The observed time evolution of the amplitude shows that we do have a stationary solution, but the effect of the small part of the probability density that propagates is much more pronounced, and makes things look much more chaotic (figure 16). In the early time picture we can also see that these probability waves get reflected back towards the soliton (and also get reflected by the soliton). Clearly, the interesting dynamics observed here deserves further study.

We also note similar structure in the oscillations from one backbone to the next, see figure 17. The oscillations are more pronounced, and their envelope is probably due to the probability bouncing from the boundaries. The fastest oscillation is then, almost certainly, the frequency of the breather.

The sharp jump of z and θ at the soliton position can again be seen in figure 18.

The situation changes drastically if we increase J to 0.04. We still have a well defined relaxation, figure 19, but there is no longer a stable soliton.

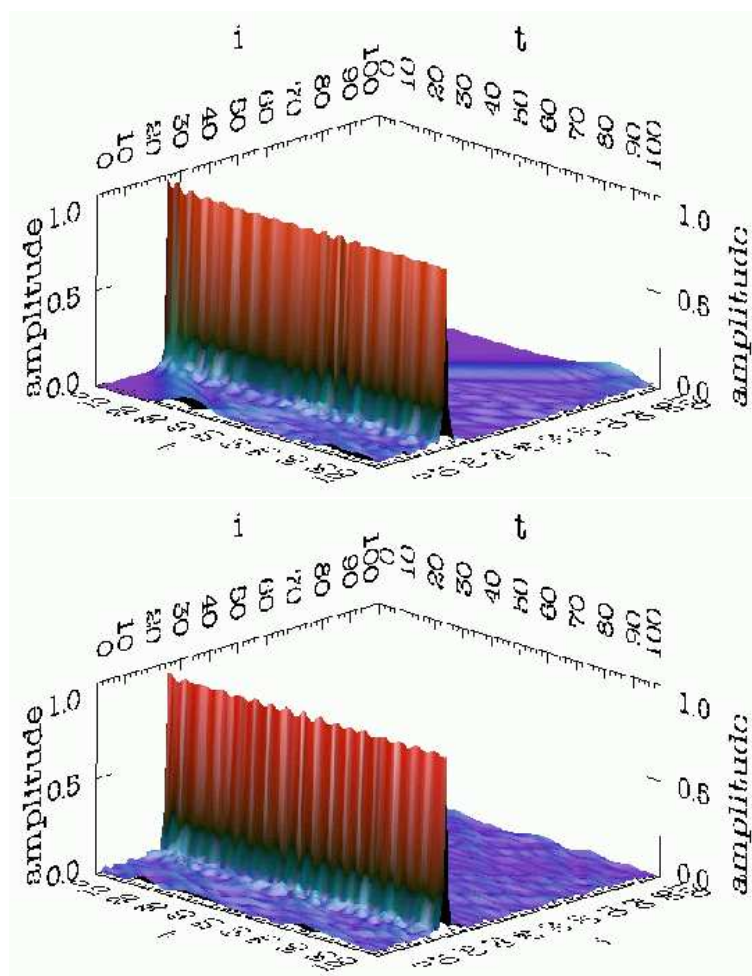


Figure 12. Time evolution of the occupation as a function of the position along the backbone (sum over both) for $J = 0.02$. t gives a time slice number (100 slices used for each figure). The top figure shows the early time evolution, the lower one the late time steady state breather solution. A dynamical representation of the evolution is available at <http://walet.phy.umist.ac.uk/DNA/Jp02.php>.

In figure 20 we demonstrate this. We note a fast decay of the soliton, even before the reflected waves have a chance to return to it. This suggests the absence of a stable breather. At later times, as shown in the lower panel, we see that a soliton-like structure gets reassembled at a different position. This may well indicate that at this point the solitons are only marginally unstable.

The envelope of the norm also shows more structure, even though this structure seems to be overlaid on a very regular pattern, figure 21.

The coupling to the position of the mechanical structure of the double helix is substantial, as can be seen from the results shown in figure 22.

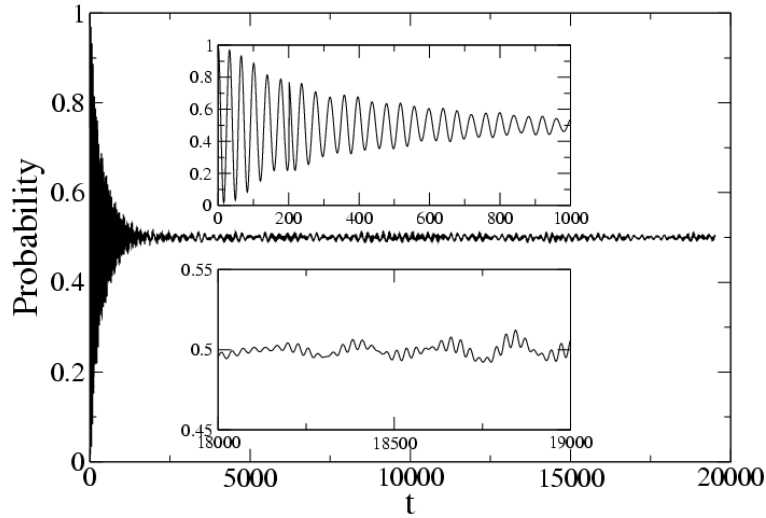


Figure 13. Time evolution of the total occupation of one of the backbones as a function of time for $J = 0.02$. The insets show both early and late oscillations of this quantity.

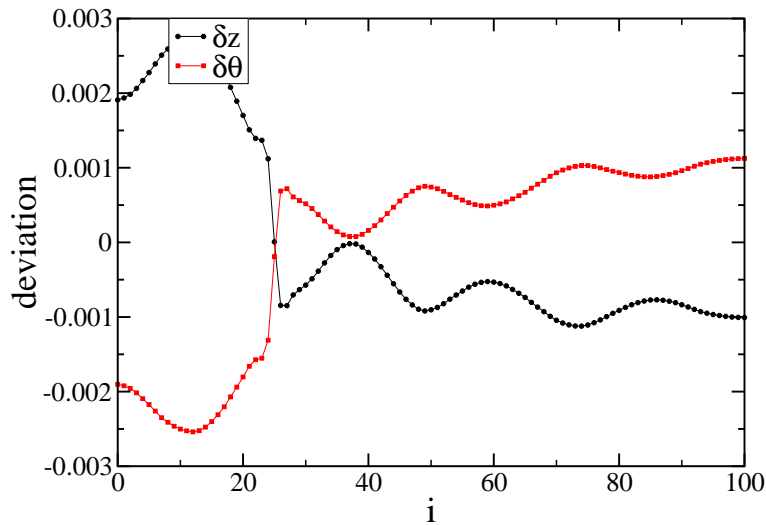


Figure 14. Deviation of θ (red squares) and z (black circles) from their equilibrium values for the final simulation point, $t = 19318$, as a function of the lattice point labelled by i . The coupling parameter $J = 0.02$.

5. Conclusions

We have constructed a model that describes the chiral movement of electrons in a double helix. We have shown how it describes both localised and delocalised charge, depending on parameters.

We have shown that the dynamics of a chiral molecule chain can be quite involved and interesting, leading to a complicated interplay of stretching and twisting modes of the underlying double helix generated by the movement of the electrons. As J_0

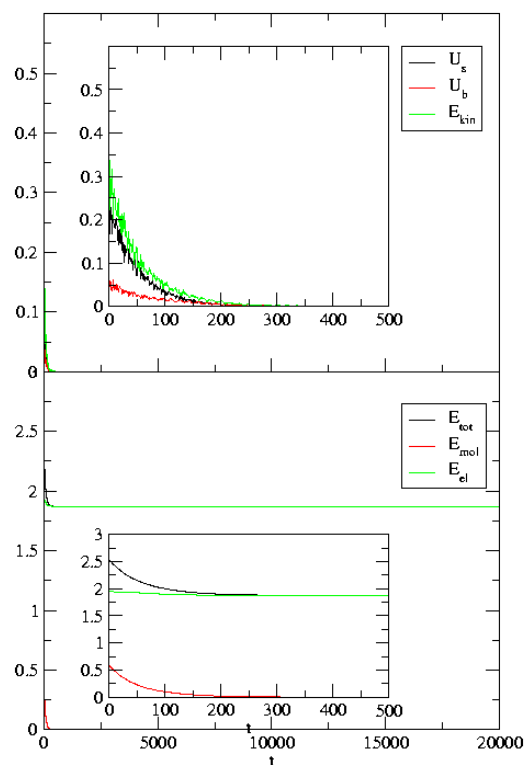


Figure 15. Energetics of the relaxation of a 101-rung chain for $J = 0.03$. The upper panel with inset shows the decrease of the mechanical energy, the lower panel the decrease of the total and the electronic energy.

increases the system exhibits a sharp transition from localised solitons (charge density) to a completely delocalised system with a complicated temporal structure. In each case we see an anticorrelation between z and θ , with the soliton deforming the lattice by locally reducing the spacing of the double helix and increasing its twist.

Our next step will be to try to extend these calculations to charge transport, where electrons come in on one backbone at one end, and leave through the same or the other backbone at the other side.

Acknowledgments

The authors acknowledge support by the EPSRC under grants GR/N28320/01 (WJZ) and GR/N15672 (NRW). One of the authors (NRW) is grateful for hospitality at the Department of Mathematical Sciences, University of Durham, which contributed greatly to this paper.

- [1] Watson, J and Crick, F 1953 A structure for Deoxyribose Nucleic Acid *Nature (London)* **171** 737–738.
- [2] Richter, J, Mertig, M, Pompe, W, Monch, I, and Schackert, H K 2001 Construction of highly conductive nanowires on a DNA template *Appl. Phys. Lett.* **78** 536–538.
- [3] Joshi, H S and Tor, Y 2001 Metal-containing DNA hairpins as hybridization probes *Chem. Commun.* 549–550.

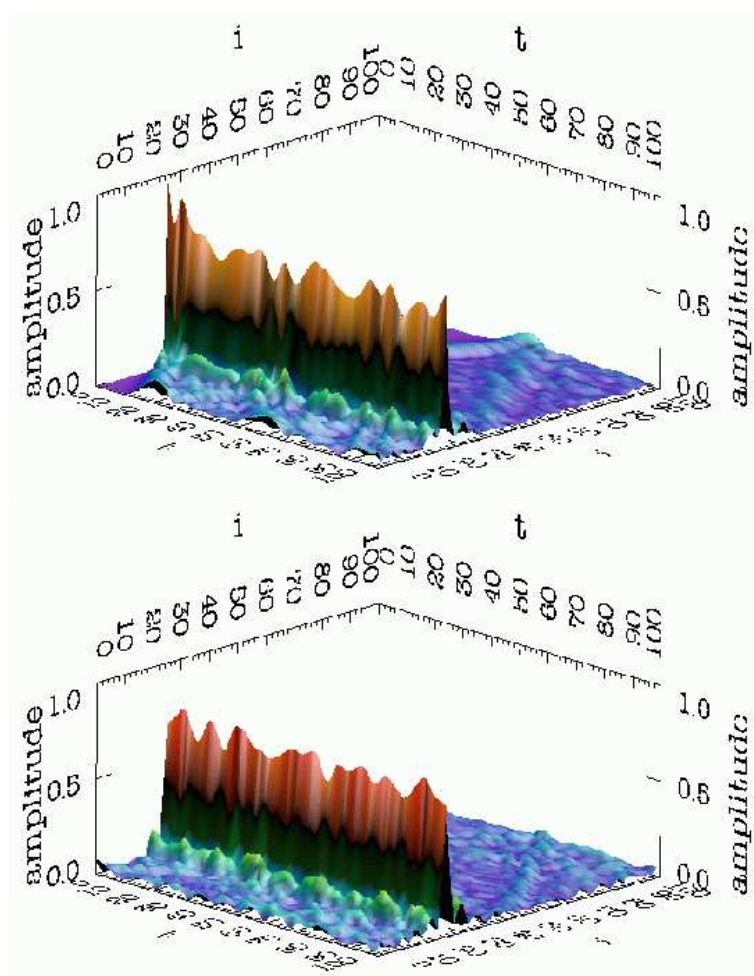


Figure 16. Time evolution of the occupation of the site as a function of the position along the backbone (sum over both) for $J = 0.03$. t gives a time slice number (100 slices used for each figure). The top figure shows the early time evolution, the lower one the late time steady state breather solution. A dynamical representation of the evolution is available at <http://walet.phy.umist.ac.uk/DNA/Jp03.php>.

- [4] Aich, P, Skinner, R J S, Wettig, S D, Steer, R P, and Lee, J S 2002 Long range molecular wire behaviour in a metal complex of DNA *J. Biomol. Struct. Dyn.* **20** 93–98.
- [5] Richter, J 2003 Metallization of DNA *Physica E* **16** 157–173.
- [6] Porath, D, Bezryadin, A, de Vries, S, and Dekker, C 2000 Direct measurement of electrical transport through DNA molecules *Nature* **493** 635–639.
- [7] Storm, A J, van Noort, J, de Vries, S, and Dekker, C 2001 Insulating behavior for DNA molecules between nanoelectrodes at the 100 nm length scale *Appl. Phys. Lett.* **79** 3881–3883.
- [8] Cuniberti, G, Craco, L, Porath, D, and Dekker, C 2002 Backbone-induced semiconducting behavior in short DNA wires *Phys. Rev. B* **65** 241314.
- [9] Yakushevich, L V 1998 *Nonlinear Physics of DNA* (Wiley: Chichester).
- [10] Peyrard, M 2004 Nonlinear dynamics and statistical physics of DNA *Nonlinearity* **17** R1–R40.
- [11] Christiansen, P L, Gaididei, Y B, and Mingaleev, S F 2001 Effects of finite curvature on soliton dynamics in a chain of non-linear oscillators *J. Phys.-Cond. Matt.* **13** 1181–1192.
- [12] Mingaleev, S F, Christiansen, P L, Gaididei, Y B, Johansson, M, and Rasmussen, K O 1999 Models for energy and charge transport and storage in biomolecules *J. Biol. Phys.* **25** 41–63.

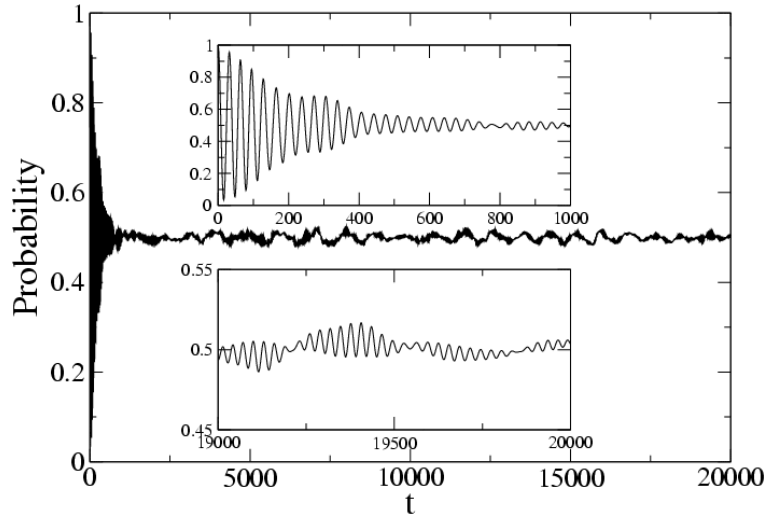


Figure 17. Time evolution of the total occupation of one of the backbones as a function of time for $J = 0.03$.

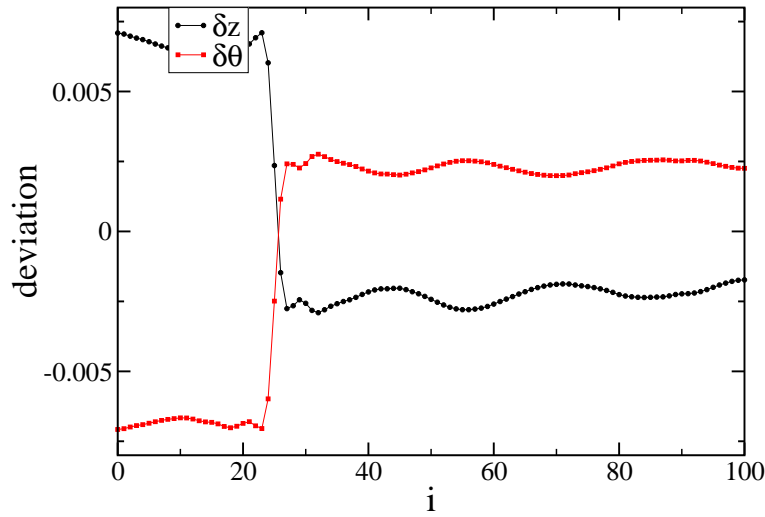


Figure 18. Deviation of θ and z from their equilibrium values for the final simulation time, $t = 19395$, as a function of the lattice point label i and $J = 0.03$.

- [13] Agarwal, J and Hennig, D 2003 Breather solutions of a nonlinear DNA model including a longitudinal degree of freedom *Physica A* **323** 519–533.
- [14] Cuevas, J, Palmero, F, Archilla, J F R, and Romero, F R 2003 Interaction of moving localized oscillations with a local inhomogeneity in nonlinear Hamiltonian Klein-Gordon lattices *Th. Mat. Phys.* **137** 1406–1411.
- [15] Dong, R X, Yan, X L, Pang, X F, and Liu, S G 2003 The nonlinear characteristics study of the effect of salt on denaturation transition of DNA *Acta Phys. Sin.* **52** 3197–3202.
- [16] Hadzievski, L, Stepic, M, and Skoric, M M 2003 Modulation instability in two-dimensional nonlinear Schrodinger lattice models with dispersion and long-range interactions *Phys. Rev. B* **68** 014305.
- [17] Hennig, D, Archilla, J F R, and Agarwal, J 2003 Nonlinear charge transport mechanism in periodic and disordered DNA *Physica D* **180** 256–272.

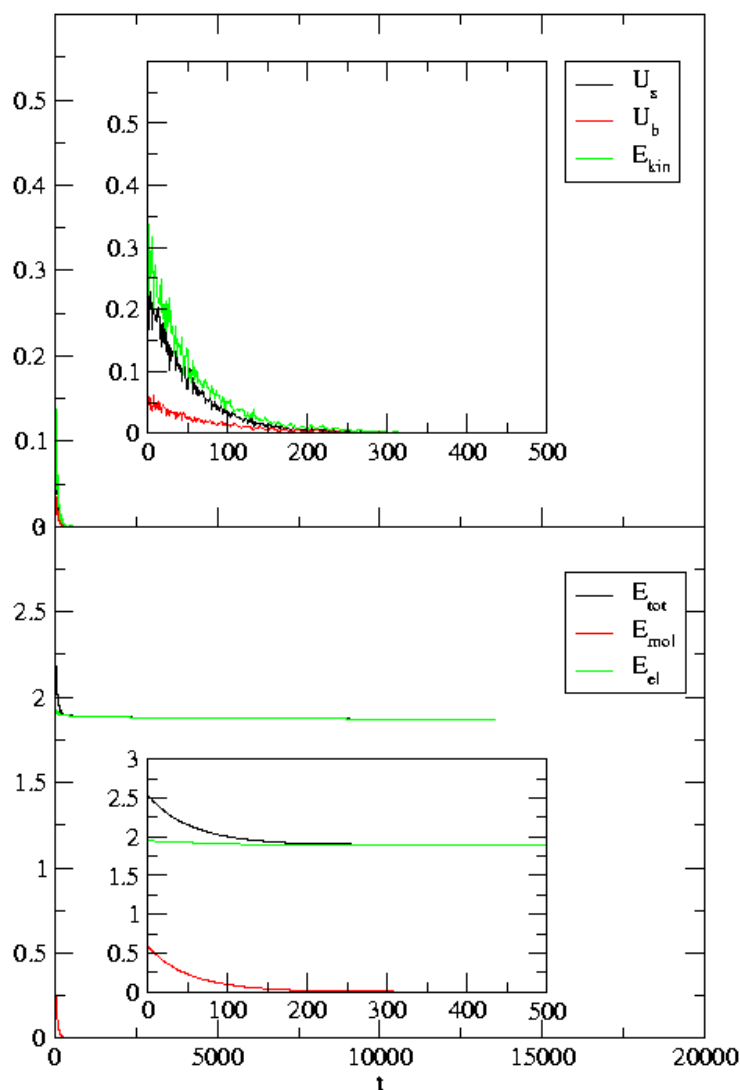


Figure 19. Energetics of the relaxation of a 101-rung chain for $J = 0.04$. The upper panel with inset shows the decay of the mechanical energy, the lower panel the decay of the total and electronic energies

- [18] Iguchi, K 2003 Extrinsic semiconductor character of a double strand of DNA: Holstein's polarons as donors and acceptors *Int. J. Mod. Phys. B* **17** 2565–2578.
- [19] Kalosakas, G and Bishop, A R 2003 Intrinsic inhomogeneity due to nonlinearity *Physica B* **338** 87–91.
- [20] Kevrekidis, P G 2003 On a class of discretizations of Hamiltonian nonlinear partial differential equations *Physica D* **183** 68–86.
- [21] Kevrekidis, P G and Weinstein, M I 2003 Breathers on a background: periodic and quasiperiodic solutions of extended discrete nonlinear wave systems *Math. Comp. Simul.* **62** 65–78.
- [22] Maniadis, P, Kalosakas, G, Rasmussen, K O, and Bishop, A R 2003 Polaron normal modes in the Peyrard-Bishop-Holstein model *Phys. Rev. B* **68** 174304.
- [23] Papacharalampous, I E, Kevrekidis, P G, Malomed, B A, and Frantzeskakis, D J 2003 Soliton collisions in the discrete nonlinear Schrodinger equation *Phys. Rev. E* **68** 046604.
- [24] Endres, R G, Cox, D L, and Singh R R P 2004 Colloquium: The quest for high-conductance DNA

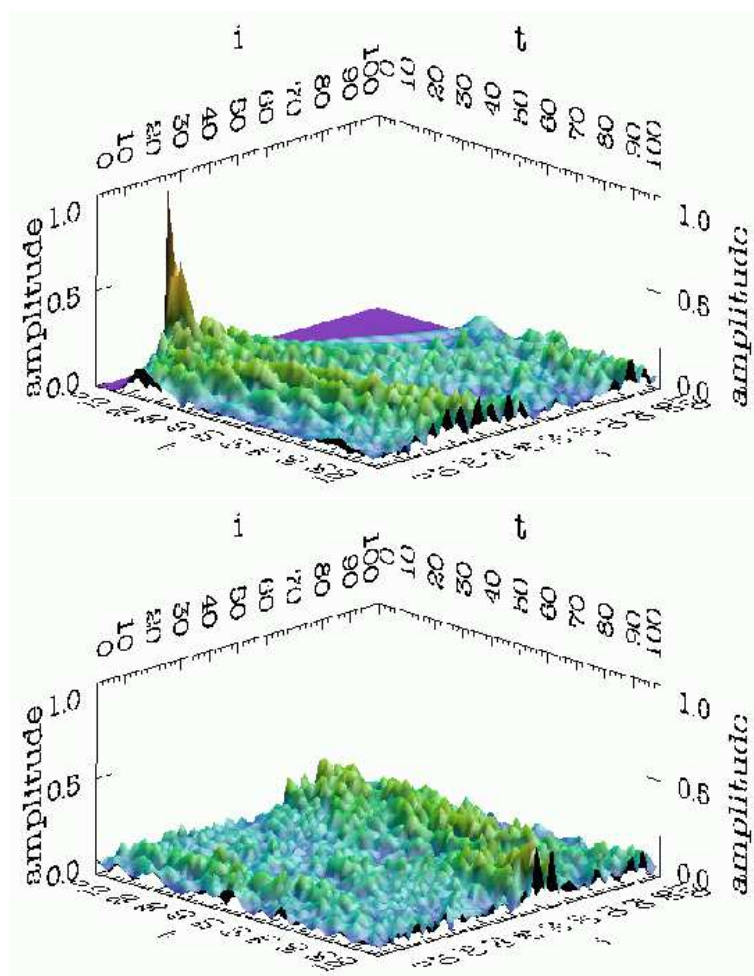


Figure 20. Time evolution of the occupation as a function of the position along the backbone (summed over both) for $J = 0.04$. t gives a time slice number (100 slices used for each figure). The top figure shows the early time evolution, the lower one the late time “chaos”. A dynamical representation of the evolution is available at <http://walet.phy.umist.ac.uk/DNA/Jp04.php>.

Rev. Mod. Phys. **76** 195.

- [25] Hartmann, B and Zakrzewski, W J 2002 Solitons and deformed lattices I cond-mat/0211239.
- [26] Eley, D D and Spivey, D I 1962 Semiconductivity of organic substances. IX. Nucleic acid in the dry state *Trans. Faraday Soc.* **58** 411–415.
- [27] Calladine, C R and Drew, H R 1997 *Understanding DNA: the molecule and how it works* 2nd ed. (Academic Press: San Diego).
- [28] Levitt, M 1983 Computer simulation of DNA double-helix dynamics, in: *Cold Spring Harbor Symposia on Quantative Biology*, vol. XLVII (Cold Spring Harbor Laboratory Press: Cold Spring Harbor, NY) pp. 251–262.
- [29] Eilbek, J C and Johansson, M 2002 The discrete nonlinear Schrödinger equation-20 years on, in *Proceedings of the conference on localization and energy transfer in nonlinear systems, San Lorenzo de El Escorial* (World Scientific: Singapore)

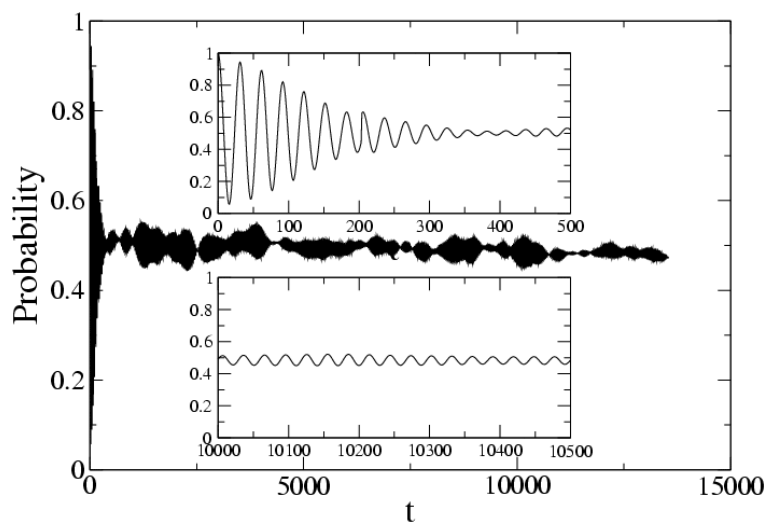


Figure 21. Time evolution of the total occupation of one of the backbones as a function of time for $J = 0.04$.

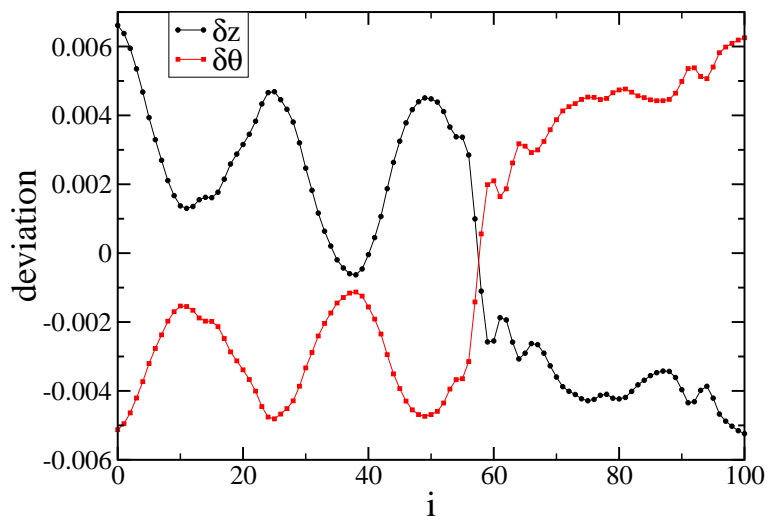


Figure 22. Deviation of θ and z from their equilibrium values for the final simulation time, $t = 13339.5$, as a function of the lattice point label i and $J = 0.04$.